Journal of Ceramic Processing Research. Vol. 11, No. 4, pp. 498~502 (2010)

J O U R N A L O F
Ceramic Processing Research

Properties and rapid consolidation of binderless nanostuctured tantalum carbide by pulsed current activated sintering

In-Jin Shon[a,b], Byung-Ryang Kim[a], In-Yong Ko[a,*], Kee-Seok Nam[c] and Jung-Mann Doh[d]

[a]*Division of Advanced Materials Engineering and the Research Center of Advanced Material Development, Engineering College, Chonbuk National University, 561-756, Republic of Korea*

[b]*Department of Hydrogen and Fuel Cells Engineering, Specialized Graduate School, Chonbuk National University, 561-756, Republic of Korea*

[c]*Korea Institute of Materials Science 531 Changwondaero, Changwon, Gyeongnam, 641-831, Korea*

[d]*Advanced Functional Materials Research Center, Korea Institute of Science and Technology, PO Box 131, Cheongryang, Seoul 130-650, Republic of Korea*

The grain size of TaC decreases with an increase in ball mliing time. Nanopowder of TaC was fabricated by high energy ball milling for 10 h. A densely pure TaC hard material with a relative density of up to 96% was produced with simultaneous application of 80 MPa pressure and pulsed current within 2 minutes. The density and hardness of TaC increased with a decrease in the initial TaC powder size. The fracture toughness and hardness values of TaC obtained from 10 h milled powder were 6.8 MPa·m$^{1/2}$ and 2076 kg/mm^2, respectively under 80 MPa pressure and with a pulsed current of 2800A.

Key words: Sintering, Nanophase, Hardness, Toughness, TaC.

Introduction

Refractory metal carbides are promising ceramic materials, because these compounds exhibit unusual combinations of physical and chemical properties such as high hardness, high melting point and excellent resistance to oxidation [1]. Industrial applications of the carbides are in cutting tools and hard coatings. Furthermore, due to their optical, electronic and magnetic properties, the carbides have been used for optical coatings, electrical contacts and diffusion barriers [2]. Among these carbides, tantalum monocarbide TaC has a NaCl type structure and is characterized by a high hardness, high melting point (3880 °C), good electrical conductivity (42.1 μΩ at 25 °C), good resistance to chemical attack and thermal shock, and excellent resistance to oxidation [3]. These properties make it very attractive for high-temperature and electronic application.

Nanocrystalline materials have received much attention as advanced engineering materials with improved physical and mechanical properties [4, 5]. Since nanomaterials possess high strength, high hardness, excellent ductility and toughness, undoubtedly, more attention has been paid to the application of nanomaterials [6-8]. In recent days, nanocrystalline powders have been developed by the thermochemical and thermomechanical process named the spray conversion process (SCP), co-precipitation and high energy milling [9-11]. However, the grain size in sintered materials becomes much larger than that in pre-sintered powders due to the fast grain growth during a conventional sintering process. Therefore, even though the initial particle size is less than 100 nm, the grain size increases rapidly up to 500 nm or larger during conventional sintering [12]. So, controlling grain growth during sintering is one of the keys to the commercial success of nano-structured materials. In this regard, pulsed current activated sintering (PCAS) which can make dense materials within 2 minutes has been shown to be effective in achieving this goal [13, 14].

In this study, we investigated the sintering of TaC without the use of a binder by the PCAS method. The goal of this research is to produce nanopowder and dense binderless nanostructured TaC hard material. In addition, we also studied the effect of high energy ball milling on the sintering behavior and mechanical properties of binderless TaC.

Experimental procedures

The tantalum carbide powder with a grain size of −325 mesh and 99.5% purity used in this research was supplied by Alfa. The powder was first milled in a high-energy ball mill (Pulverisette-5 planetary mill) at 250 rpm for various periods of time (0, 1, 4, 10 h). Tungsten carbide balls (8.5 mm in diameter) were used in a sealed cylindrical stainless steel vial under an argon atmosphere. The weight ratio of balls-to-powder was 30 : 1. Milling resulted in a significant reduction of the grain size. The grain sizes of the TaC was calculated from the full width at half-maximum

*Corresponding author:
Tel : +82-63-270-2295
Fax: +82-63-270-2386
E-mail: plasma@chonbuk.ac.kr

(FWHM) of a diffraction peak by Suryanarayana and Grant Norton's formula [15].

$$B_r\ (B_{crystalline} + B_{strain})\ \cos\theta = k\ \lambda/L + \eta\sin\theta \qquad (1)$$

where B_r is the full width at half-maximum (FWHM) of the diffraction peak after instrumental correction; $B_{crystalline}$ and B_{strain} are FWHM caused by a small grain size and internal stress, respectively; k is constant (with a value of 0.9); λ is the wavelength of the X-ray radiation; L and η are the grain size and internal strain, respectively; and θ is the Bragg angle. The parameters B and B_r follow Cauchy's form with the relationship: $B = B_r + B_s$, where B and B_s are FWHM of the broadened Bragg peaks and the standard sample's Bragg peaks, respectively. The average grain sizes of the TaC milled for 1, 4 and 10 h determined by Suryanarayana and Grant Norton's formula were about 31 nm, 20 nm and 15 nm, respectively.

The powders were placed in a graphite die (outside diameter, 45 mm; inside diameter, 20 mm; height, 40 mm) and then introduced into the pulsed current activated sintering (PCAS) apparatus shown schematically in Fig. 1. The PCAS apparatus includes a 30 kW power supply which provides a pulsed current (on time; 20 μs, off time; 10 μ) through the sample, and a 50 kN uniaxial load. The system was first evacuated and a uniaxial pressure of 80 MPa was applied. A pulsed current was then activated and maintained until the densification rate was negligible, as indicated by the real-time output of the shrinkage of the sample. The shrinkage was measured by a linear gauge measuring the vertical displacement. Temperatures were measured by a pyrometer focused on the surface of the graphite die. At the end of the process, the induced current was turned off and the sample cooled to room temperature. The process was carried out under a vacuum of 4×10^{-2} Torr (5.33 Pa).

The relative density of the sintered sample was measured by the Archimedes method. Microstructural information was obtained from product samples, which had been polished and etched using Murakami's reagent (10 g potassium ferricyanide, 10 g NaOH, and 100 mL water) for 1-2 minutes at room temperature. Compositional and microstructural analyses of the products were made through X-ray diffraction (XRD), scanning electron microscopy (SEM) with energy dispersive spectroscopy (EDS) and a field emission scanning electron microscope (FE-SEM). Vickers hardness was measured by performing indentations at a load of 20 kg_f and a dwell time of 15 s.

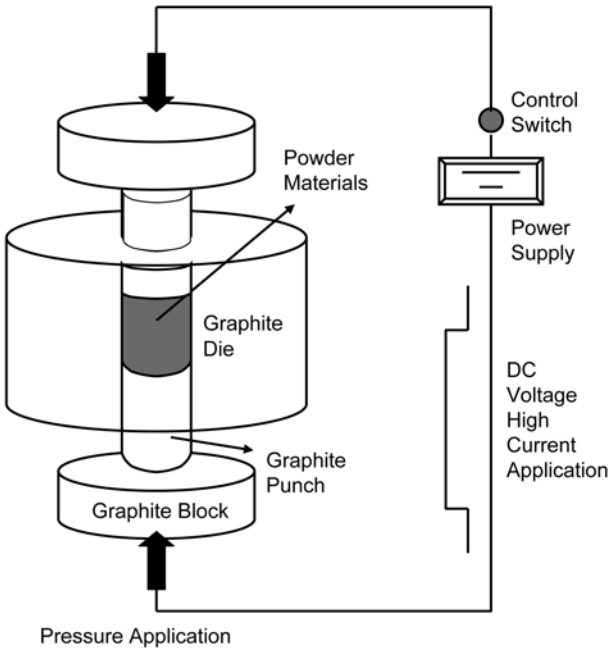

Fig. 1. Schematic diagram of the apparatus for pulsed current activated sintering.

Results and Discussion

Fig. 2 shows X-ray diffraction patterns of the TaC powder after various milling times. The full width at half-maximum (FWHM) of a diffraction peak is wider with milling time due to strain and refinement of the powder. TEM images of the TaC powder with milling time are shown in Fig. 3.

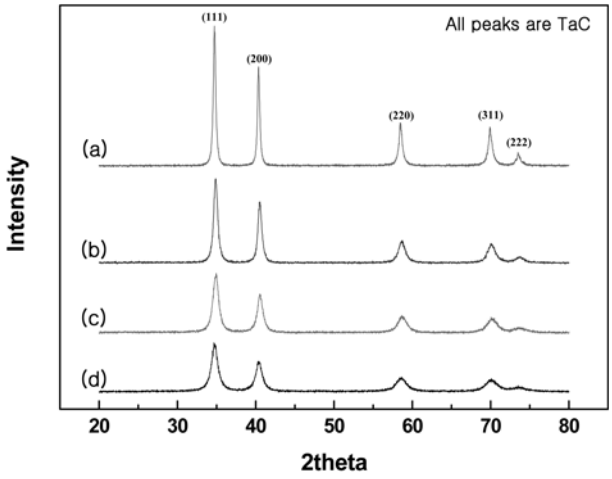

Fig. 2. X-ray diffraction patterns of the TaC powder after various milling times : (a) 0, (b) 1, (c) 4, and (d) 10 h.

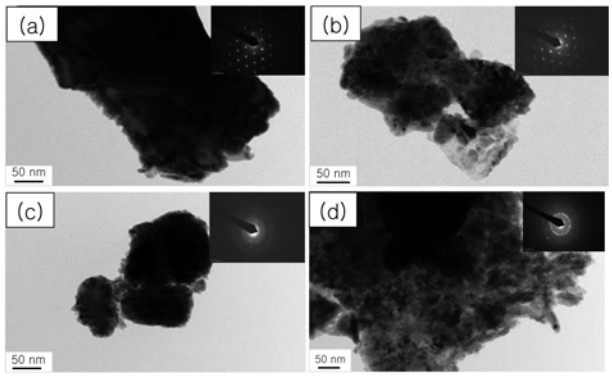

Fig. 3. TEM images of the TaC powders with milling times : (a) 0, (b) 1, (c) 4, and (d) 10 h.

TaC powder without milling has a spot pattern but the TaC powder has ring pattens after milling. The grain sizes of TaC milled for 1, 4, 10 h were 31, 20, and 15 nm, respectively. The variations of the shrinkage displacement and temperature with the heating time for a pulsed current 2800A during the sintering of the high energy ball milled TaC under a pressure of 80 MPa are shown in Fig. 4. In all cases, the application of the pulsed current resulted in shrinkage due to consolidation. The shrinkage initiation temperature varied from 1000 to 1300 °C depending on the milling time. The temperature at which shrinkage started decreased with an increase in the milling time, and the high energy ball milling affected the rate of densification and the final density, as will be discussed below. A high-energy ball milling treatment allows the control of the formation of the compound by fixing the reactant powder microstructure. Indeed, high-energy ball milling produces finer crystallites, strain and defects. Therefore, the consolidation temperature decreases with milling time because the driving force for sintering and contact points of powders for atomic diffusion increases. Fig. 5 shows SEM images of TaC sintered from various milled powders and a FE-SEM image of TaC sintered from the 10 h milled powder is shown in Fig. 6. From the figures, it is known that the TaC is consisted of nanoparticle. Fig. 7 shows the XRD patterns of TaC sintered for all four powders used in this study. All peaks are TaC.

A plot of B_r ($B_{crystalline} + B_{strain}$) cosθ versus sinθ in Suryanarayana and Grant Norton's formula [15] is shown in Fig. 8. The average grain sizes of the TaC calculated from the XRD data were about 627, 162, 93 and 54 nm for the samples with milling times of 0, 1, 4, and 10 h and their corresponding densities were approximately 72.

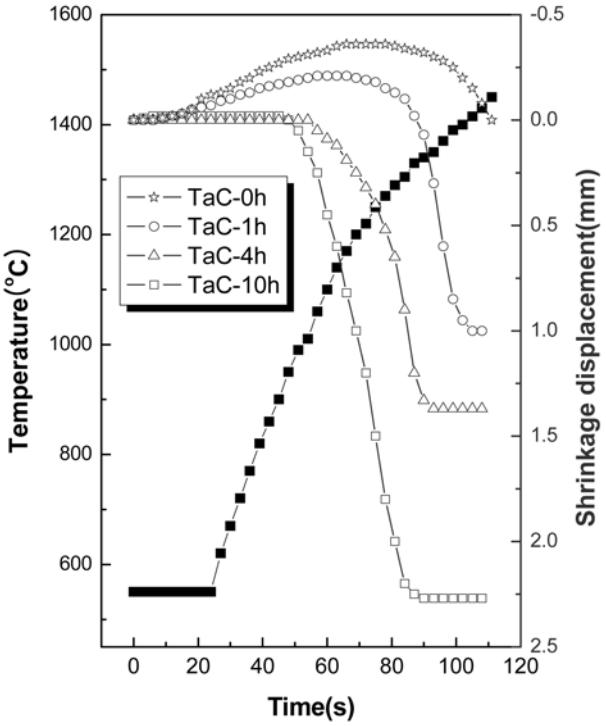

Fig. 4. Variations of temperature and shrinkage with heating time during the pulsed current activated sintering of binderless TaC with milling times of 0, 1, 4, and 10hr.

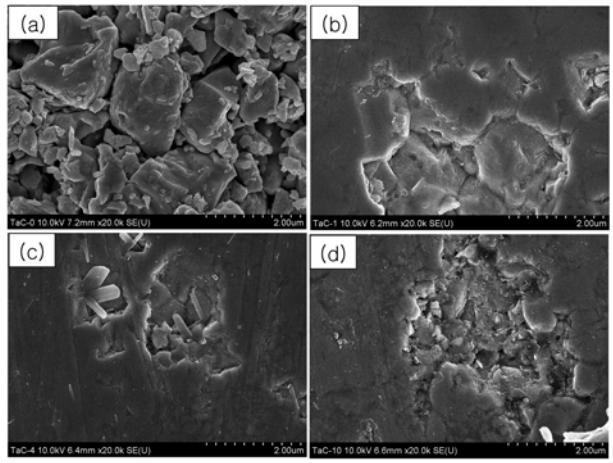

Fig. 5. SEM images of pure TaC sintered from various milled powder for : (a) 0, (b) 1, (c) 4, and (d) 10 h.

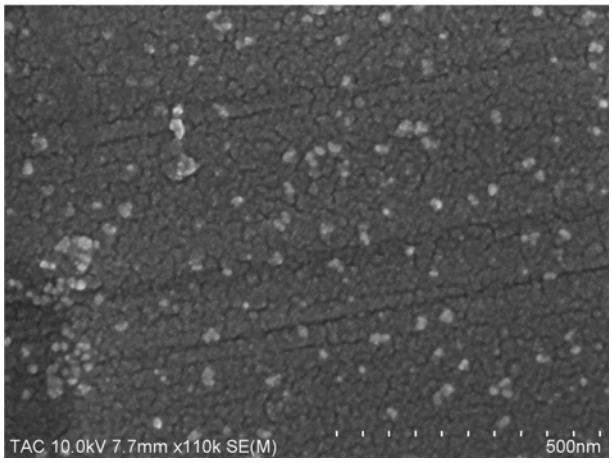

Fig. 6. FE-SEM micrograph of pure TaC sintered from the 10 h milled powder.

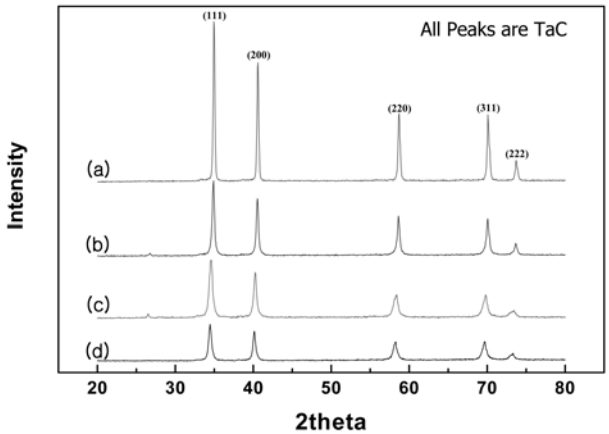

Fig. 7. XRD patterns of binderless TaC sintered from various milled powders : (a) 0, (b) 1, (c) 4, and (d) 10 h.

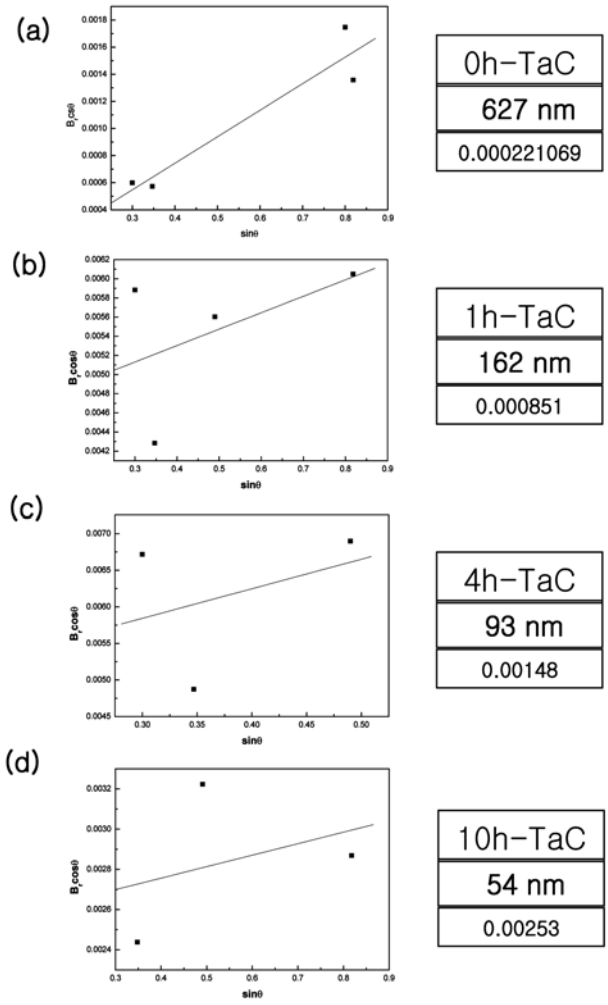

Fig. 8. Plots of B_r ($B_{crystallite} + B_{strain}$) cosè versus sinè for TaC sintered from various milled powders : (a) 0, (b) 1, (c) 4, and (d) 10 h.

87, 91 and 96%, respectively. Thus, the average grain size of the sintered TaC is not greatly larger than that of the initial powder, indicating the absence of much great grain growth during sintering. This retention of the grain size is attributed to the high heating rate and the relatively short term exposure of the powders to the high temperature.

The role of the current (resistive or inductive) in sintering has been the focus of several attempts aimed at providing an explanation of the observed enhancement of sintering and the improved characteristics of the products. The role played by the current has been variously interpreted, the effect being explained in terms of a fast heating rate due to Joule heating, the presence of a plasma in pores separating powder particles [16], and the intrinsic contribution of the current to mass transport [17-19].

Vickers hardness measurements were performed on polished sections of the TaC samples using a 20 kg_f load and 15 s dwell time. Indentations with large enough loads produced radial cracks emanating from the corners of the indent. The length of these cracks permits the fracture toughness of the material to be estimated using the formula due to Anstis et al [20],

$$K_{IC} = 0.016(E/H)^{1/2}P/C^{3/2} \quad (2)$$

where E is Young's modulus, H is the indentation hardness, P is the indentation load, and C is the trace length of the crack measured from the center of the indentation.

The Vickers hardnesses of the TaC with ball milling for 1, 4 and 10 h were 1287 $kg{\cdot}mm^{-2}$, 1645 $kg{\cdot}mm^{-2}$ and 2076$\cdot kg{\cdot}mm^{-2}$, and their fracture toughnesses were 8 $MPa{\cdot}m^{1/2}$, 7.1 $MPa{\cdot}m^{1/2}$ and 7 $MPa{\cdot}m^{1/2}$, respectively. These values represent the average of ten measurements. The hardness of TaC with ball milling for 10 h is very high with a high fracture toughness due to refinement of grain.

Summary

Nanopowder of TaC was fabricated by high energy ball milling. Using the rapid sintering method, PCAS, the densification of binderless TaC was accomplished using high energy ball milling. The consolidation temperature decreased with milling time because the driving force for sintering and contact points of powders for atomic diffusion increased. The average grain sizes of the TaC were about 627, 162, 93 and 54 nm for the samples with milling times of 0, 1, 4, and 10 h and their corresponding densities were approximately 72. 87, 91 and 96%, respectively. The Vickers hardnesses of the TaC with ball milling for 1, 4 and 10 h were 1287 $kg{\cdot}mm^{-2}$, 1645 $kg{\cdot}mm^{-2}$ and 2076 $kg{\cdot}mm^{-2}$, and their fracture toughnesses were 8 $MPa{\cdot}m^{1/2}$, 7.1 $MPa{\cdot}m^{1/2}$ and 7 $MPa{\cdot}m^{1/2}$, respectively.

Acknowledgements

"We are grateful for the financial support from the Korea Institute of Science and Technology, which was provided through the program for study on Development of Surface Treatment for Light Metals".

References

1. O.Y. Khyzhun, E.A. Zhurakovsky, A.K. Sinelnichenko and V.A. Kolyagin, J. Electron Spectrosc. Relat. Phenom. 82 (1996) 179-185.
2. S.T. Oyama, Introduction to the chemistry of transition metal carbides and nitrides in : S. T. Oyama (Ed.), Blackie Academic and Professional (1996).
3. Y.J. Chen, J.B. Li, Q.M. Wei and H.Z. Zhai, Mater. Lett. 56 (2002) 279-284.
4. H. Suzuki et al., Cemented Carbide and Sintered Hard Materials, Maruzen, Tokyo, (1986).
5. M. Sherif El-Eskandarany, J. Alloys & Compounds 305 (2000) 225-230.
6. L. Fu, L.H. Cao and Y.S. Fan, Scripta Materialia 44 (2001) 1061-1065.
7. K. Niihara and A. Nikahira, Advanced structural Inorganic Composite, Elsevier Scientific Publishing Co., Trieste, Italy, (1990).
8. S. Berger, R. Porat and R. Rosen, Progress in Materials 42, (1997) 311-322.
9. Z. Fang and J.W. Eason, Int. J. of Refractory Met. & Hard

Mater. 13 (1995) 297-302.
10. I.J. Shon, D.K. Kim, K.T. Lee and K.S. Nam, Metals and Materials International 5 (2008) 593-598.
11. B.R. Kim, K.S. Nam, J.K. Yoon, J.M. Doh, K.T. Lee and I.J. Shon, J. Ceramic Processing Research 10 (2009) 171-176.
12. M. Sommer, W.D. Schubert, E. Zobetz and P. Warbichler, Int. J. of Refractory Met. & Hard Mater. 20 (2002) 41-46.
13. I.J. Shon, D.K. Kim, K.T. Lee, K.S. Nam, Metals and Materials International 14 (2008) 593-598.
14.. S.K Bae, I.J. shon, J.M doh, J. K. Yoon, I.Y. Ko, Scripta Materialia 58 (2008) 425-429.
15. C. Suryanarayana and M. Grant Norton, X-ray Diffraction A Practical Approach, Plenum Press, New York, (1998).
16. Z. Shen, M. Johnsson, Z. Zhao and M. Nygren, J. Am. Ceram. Soc. 85 (2002) 1921-1927.
17. J.E. Garay, U. Anselmi-Tamburini, Z.A. Munir, S.C. Glade and P. Asoka- Kumar, Appl. Phys. Lett. 85 (2004) 573-577.
18. J.R. Friedman, J.E. Garay. U. Anselmi-Tamburini and Z.A. Munir, Intermetallics. 12 (2004) 589-596.
19. J.E. Garay, J.E. Garay. U. Anselmi-Tamburini and Z.A. Munir, Acta Mater., 51 (2003) 4487-4493.
20. G.R. Anstis, P. Chantikul, B.R. Lawn and D.B. Marshall, J. Am. Ceram. Soc. 64 (1981) 533-539.